

## 晶面选择性生长对球形氢氧化镍形貌及电化学活性的影响

唐俊杰 刘 燕\* 田 磊 张丽丽 王东兴 张延安  
(东北大学多金属共生矿生态化冶金教育部重点实验室, 沈阳 110819)

**摘要:** 在相同的物理化学条件、不同晶化时间的条件下, 采用化学沉淀法制备球形氢氧化镍晶体并应用 SEM 技术分别考察制得样品的形貌。研究表明, 在相同的物理化学条件下, 随着晶化时间的增加, 样品的微观形貌由不规则状晶体变为完整的球状晶体。结合 XRD 表征结果分析得出: (001) 晶面在晶化时间达到 3 h 时生长到了一个稳定的状态, 并不随着晶化时间的增加而有明显的变化, 但 (100) 与 (101) 晶面随晶化时间的增加继续生长, 当晶化时间达到 12 h 时氢氧化镍的相对结晶度最大, (100) 与 (101) 衍射峰强度高且峰形尖锐, 说明氢氧化镍晶体的结构规整性增强。本文还讨论了氢氧化镍生长结晶过程中晶面选择性生长对晶体形貌及电化学性能的影响。

**关键词:** 球形氢氧化镍; 晶面; 衍射峰; 相对结晶度

中图分类号: O614.81\*3 文献标识码: A 文章编号: 1001-4861(2017)02-0354-07

DOI: 10.11862/CJIC.2017.049

## Influence of Crystal Growth Direction Selectivity on Morphology and Electrochemical Activity of Spherical Nickel Hydroxide

TANG Jun-Jie LIU Yan\* TIAN Lei ZHANG Li-Li WANG Dong-Xing ZHANG Ting-An

(Key Laboratory for Ecological Utilization of Multimetallic Mineral, Ministry of Education,  
Northeastern University, Shenyang 110819, China)

**Abstract:** The spherical nickel hydroxide was synthesized by chemical precipitation method under the same physical and chemical conditions but different aging times. The morphologies of the spherical nickel hydroxide were characterized by SEM. It was found that with the increase of the aging time, the morphology of the spherical nickel hydroxide changed from irregular crystals to regular spherical crystals. XRD patterns showed that when the aging time was 3 h, the growth of (001) crystal plane reached a steady state, and it did not transform with the increase of the aging time. However, (100) crystal plane and (101) crystal plane continued to grow with the increase of the aging time, and the relative crystallinity reached a maximum value. The shapes of the diffraction peaks were sharp and high when the aging time was 12 h, which indicated that the structural regularity strengthened. The influence of crystal growth direction selectivity on the morphology and electrochemical activity were discussed in the crystallization process of spherical nickel hydroxide.

**Keywords:** spherical nickel hydroxide; crystal plane; diffraction peak; relative crystallinity

Spherical  $\text{Ni}(\text{OH})_2$  is one of the most important battery material which has been widely applied in electroplating, storage battery, spaceflight and so on.

Although spherical  $\text{Ni}(\text{OH})_2$  has been industrially produced in large-scale, the structures in different batches always appear different because the growth

收稿日期: 2016-09-07。收修改稿日期: 2016-12-08。

国家自然科学基金云南联合重点基金(No.U1402271, U1202274)资助项目。

\*通信联系人。E-mail: liuyan@smm.neu.edu.cn

mechanism of  $\text{Ni}(\text{OH})_2$  crystal has not been researched thoroughly. Wang summarized the mechanism of crystal growth defect in detail. He concluded that the sub-step theory could be applied to explain the crystal growth mechanisms of both solution and sublimation processes<sup>[1-2]</sup>. Ma et al. measured and estimated crystal plane growth kinetics. They presented a framework which integrated the various components to achieve the ultimate objective of model-based closed-loop control of the CShD<sup>[3-4]</sup>. Huo et al. proposed a synthetic image analysis strategy for in-situ crystal size measurement and shape identification for monitoring crystallization processes, based on a real-time imaging system<sup>[5-7]</sup>.

X-ray diffraction plays a key role in the analysis of the crystallization process. Ramesh used XRD to determine the thermal decomposition of  $\text{Ni}(\text{OH})_2$ . Further, he concluded that the decomposition mechanism mainly depended on the preparative conditions<sup>[8]</sup>. Deschamp presented that continuing advances in all phases of a crystallographic study have expanded the ranges of samples which can be analyzed by X-ray crystallography, including larger molecules, smaller or weakly diffracting crystals, and twinned crystals<sup>[9-13]</sup>. Xu et al. used X-ray diffraction to analyze the growth and phase transformation of metastable  $\beta\text{-HgI}_2$ <sup>M</sup><sup>[14-15]</sup>.

The crystallization factors of spherical  $\text{Ni}(\text{OH})_2$  on macroscopic perspective were investigated, including temperature, pH (ammonia content), reactant supersaturation, mixing intensity and paddle type as well as many other aspects<sup>[16]</sup>. However, the factors of micro-cosmic perspective are rarely studied. Therefore, in this study the spherical  $\text{Ni}(\text{OH})_2$  was synthesized by chemical precipitation method with different aging times under the same physical and chemical conditions. The morphologies and the relative crystallinities of the spherical  $\text{Ni}(\text{OH})_2$  were characterized by SEM and XRD. It is found that the crystal growth direction selectivity has a great influence on morphologies and crystallization of spherical  $\text{Ni}(\text{OH})_2$ . This work provides the rules of the growth of crystal plane according to the crystallization of spherical  $\text{Ni}(\text{OH})_2$ . It also offers a theoretical basis and experiences for reducing the

structure differences of  $\text{Ni}(\text{OH})_2$  industrial products.

## 1 Experimental

### 1.1 Preparation of spherical $\text{Ni}(\text{OH})_2$

According to the industrial process of spherical  $\text{Ni}(\text{OH})_2$  preparation, the chemical precipitation method was applied to the preparation of spherical  $\text{Ni}(\text{OH})_2$ . The reaction temperature of the system was controlled within 50~57 °C, and the pH value was controlled within 11~11.7. A certain concentration of nickel sulfate solution, ammonia and sodium hydroxide solution in a certain proportion was filled to the bottom of the reactor. Under the same physical and chemical conditions, the samples prepared with the aging times of 3, 6, 9 and 12 h, and then the samples were filtered out for measurement.

### 1.2 Instruments

The scanning electron microscope (SEM) used in this experiment was SU8010 produced by Japan Hitachi Company. The X-ray diffractometer used in this experiment was D8 Advance X Bruker ray analyzer produced by German Bruker Company. Light tube type was Cu target ( $K\alpha$ ,  $\lambda=0.154\ 06\ \text{nm}$ ). The scan range was 10°~90° with scanning speed of 2°·min<sup>-1</sup>. The electrochemical workstation used in this experiment was Biologic vsp300 produced by France Claix Company.

## 2 Results and discussion

### 2.1 SEM analysis

Under the same physical and chemical conditions, when the aging time is 3 h, the  $\text{Ni}(\text{OH})_2$  particles form irregular crystals with different sizes, the surface structure of the crystals is composed of the acicular micro-crystals, as shown in Fig.1. It is because in the early reaction, the  $\text{Ni}(\text{OH})_2$  particles form flocculent precipitates and micro-crystals under the strong agglomeration.

When the aging time is 6 h, the  $\text{Ni}(\text{OH})_2$  particles form many agglomerate crystals with similar sizes and shapes, the surface structure of these crystals is composed of many well-defined acicular micro-crystals, as shown in Fig.2. It is because the crystal

nucleuses gradually form and crystals gradually grow with the increase of the aging time under the agglomeration. The flocculent precipitates gradually fill the gaps of agglomerated particles and the quasi spherical crystals are formed. Due to the growth of layers is perpendicular to the spherical surface in the crystallization process of spherical  $\text{Ni}(\text{OH})_2$ , the surface of these quasi spherical crystals is formed by the well-defined acicular micro-crystals.

When the aging time is 9 h, the  $\text{Ni}(\text{OH})_2$  particles form spherical crystals with similar sizes, and the surface structure of these crystals is composed of many grainy micro-crystals, as shown in Fig.3. It is because the precipitates fill the gaps of agglomerated particles and the more compact spherical crystals are formed. Due to the surface of these crystals is attached of grainy micro-crystals, the precipitates continue to adhere to the surface of the crystals and

the crystals grow slowly under the agglomeration.

When the aging time is 12 h, the  $\text{Ni}(\text{OH})_2$  particles form many complete spherical crystals with a uniform size, the surface structure of these crystals is composed of many micro-crystals with clear stripes, as shown in Fig.4. It is because the agglomerated particles combine more compact, and the surface structure of these crystals grows more integrated.

## 2.2 XRD analysis

The XRD patterns of the samples with different aging times are shown in Fig.5. It can be found that the main diffraction peaks are nickel hydroxide, and other crystal items are not observed. When the aging time is 12 h, the characteristic peaks in the XRD patterns are highest, the FWHM is minimum, and the relative crystallinity is the best. If the relative crystallinity of the samples prepared at 12 h is treated as 100%, according to amorphization formula  $A = [1 -$

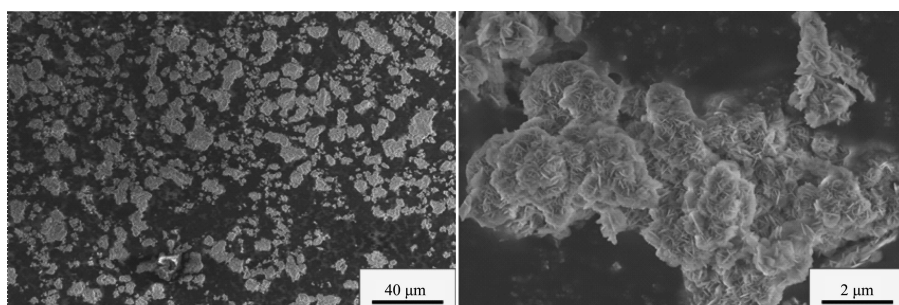


Fig.1 SEM images of  $\text{Ni}(\text{OH})_2$  particles (aging time 3 h)

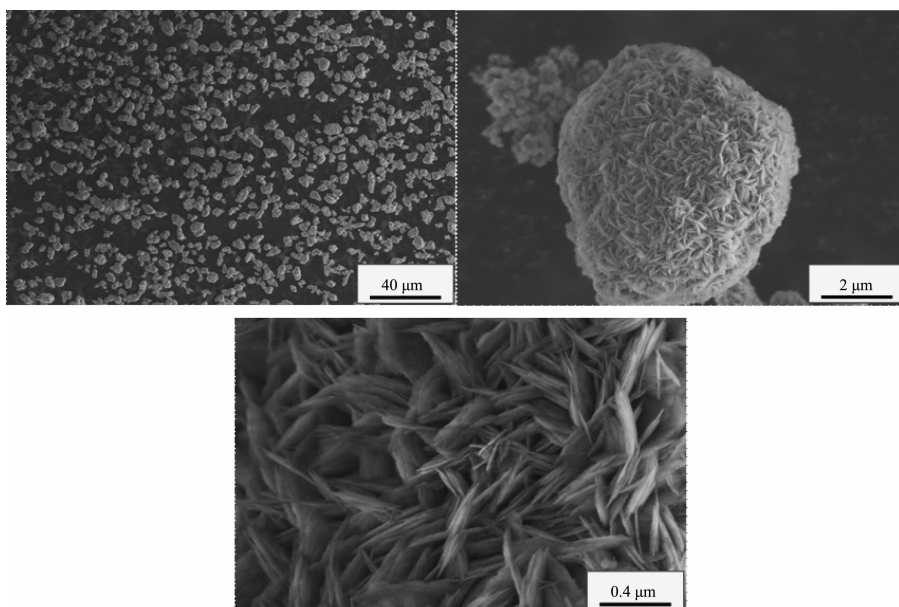
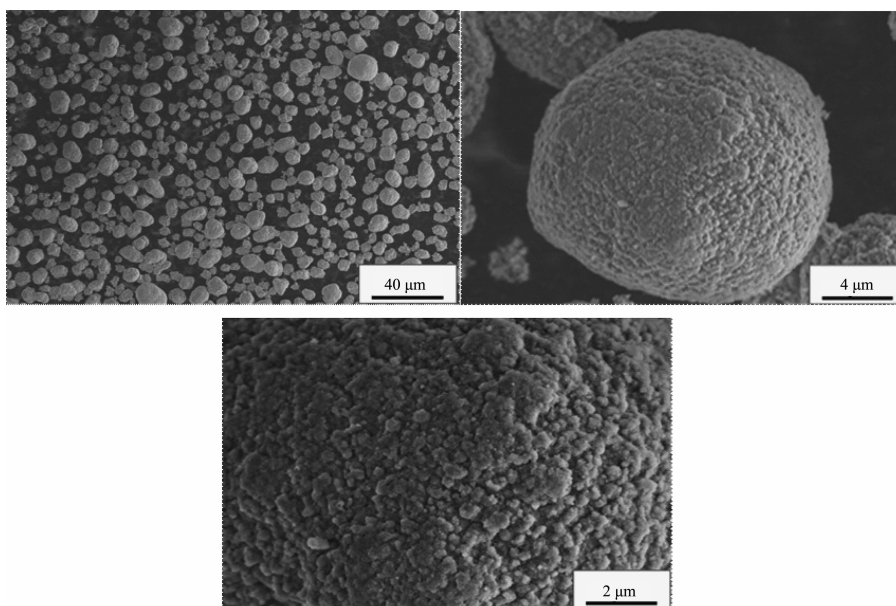
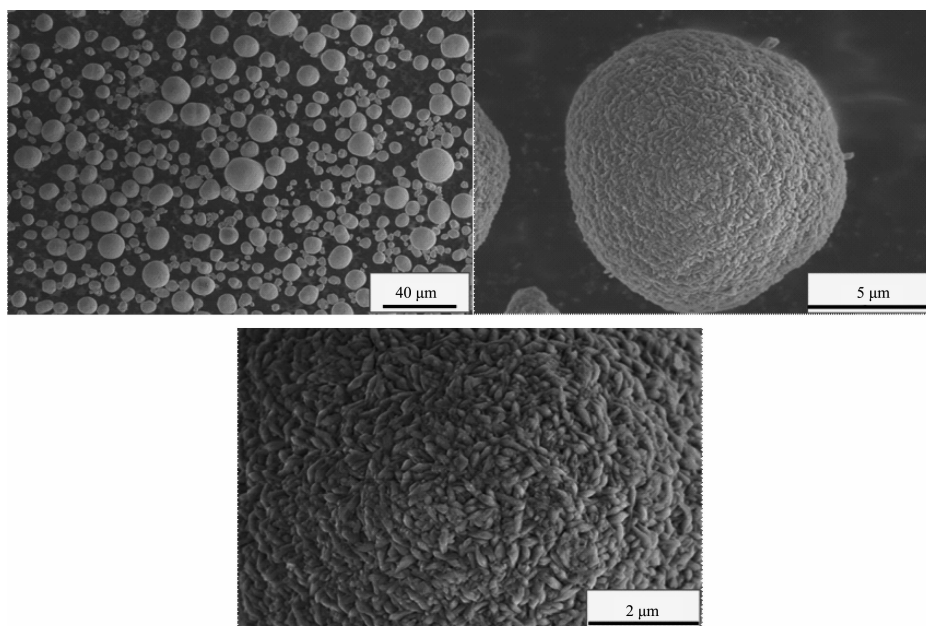


Fig.2 SEM images of  $\text{Ni}(\text{OH})_2$  particles (aging time 6 h)

Fig.3 SEM images of  $\text{Ni}(\text{OH})_2$  particles (aging time 9 h)Fig.4 SEM images of  $\text{Ni}(\text{OH})_2$  particles (aging time 12 h)

$U_{\text{ox}}/(U_{\text{x}0}) \times 100\%$ , the calculation of each samples is plotted in a linear graph, as shown in Fig.6. Moreover, the mathematical relationship between aging time and amor-phization is  $A = -0.0077T^2 + 0.0371T + 0.6532$ , which can be obtained according to Fig.6.

It can be found that the  $\text{FWHM}_{(001)}$  and the peak intensity on (001) diffraction peak are basically the same with the increase of the aging time from Fig.5. Which means that the growth of (001) crystal plane reaches a steady state when the aging time is 3 h.

However, the  $\text{FWHM}_{(100)}$  and  $\text{FWHM}_{(101)}$  decrease while the peak intensities are enhanced. Which means that (100) crystal plane and (101) crystal plane continue to grow with the increase of the aging time. SEM images show that when the aging time is increased from 3 to 12 h, the morphology of  $\text{Ni}(\text{OH})_2$  crystals changes from irregular crystals to complete spherical crystals, it can be concluded that the growth of (001) crystal face has not a greater influence on the morphology of  $\text{Ni}(\text{OH})_2$  crystals, but the growths of (100) crystal plane and



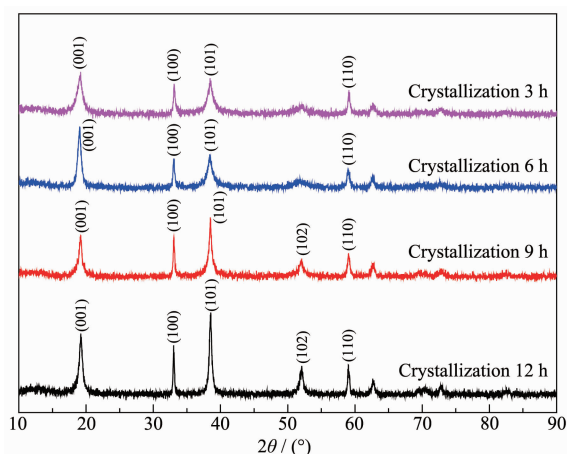


Fig.5 XRD patterns of the samples with different aging times

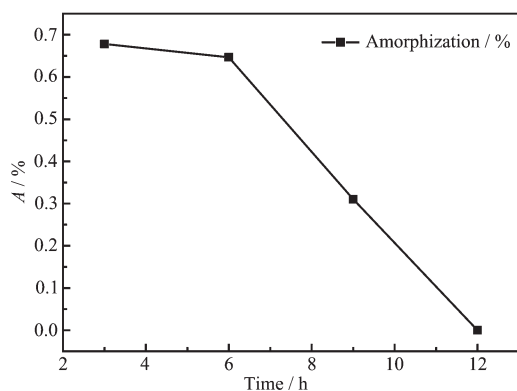


Fig.6 Aging time-conversion relation of amorphization

(101) crystal plane have a greater influence on the morphology. And the  $\text{FWHM}_{(100)}$  and  $\text{FWHM}_{(101)}$  of  $\text{Ni}(\text{OH})_2$  crystals with different aging times are given in Table 1.

According to Table 1, the selectivity of crystal

growth directions on (100) crystal plane and (101) crystal plane with different aging times can be calculated by Scherrer formula  $D = K\lambda / (B \cos \theta)$ , and the results are given in Table 2. From Table 2 it can be seen that the growth rate of (101) crystal plane is greater than (100) crystal plane when the aging time is 6~9 h, and the growth rate of (100) crystal plane is greater than (101) crystal plane when the aging time is 9~12 h. It shows from SEM images Fig.2~Fig.3 that when the aging time is increased from 6 to 9 h, the morphologies of  $\text{Ni}(\text{OH})_2$  crystals change from agglomerate crystals to spherical crystals. This means that the growth of (101) crystal plane has a greater influence on the sphericity than (100) crystal plane. SEM images Fig.3~Fig.4 show that when the aging time is increased from 9 to 12 h, the surface structures of  $\text{Ni}(\text{OH})_2$  crystals change from grainy micro-crystals to striped micro-crystals. This means that the growth of (100) crystal plane has a greater influence on the surface structure than (101) crystal plane.

### 2.3 Performance characterization

The electrochemical activity is the basic indicator of  $\text{Ni}(\text{OH})_2$ . The  $\text{Ni}(\text{OH})_2$  samples prepared at different aging times were compressed with carbon black and adhesive in proportion as 7:2:1 into sheet electrode. CV Scan was tested at the speed of 10 mA/s in the range of 0 ~ 0.6 V, while the  $\text{Hg}/\text{HgO}$  was selected as the reference electrode. The CV curves are shown in Fig.7. According to Fig.7, it can be seen

Table 1 FWHM for  $\text{Ni}(\text{OH})_2$  crystals with different aging times

Aging time / h	3	6	9	12
FWHM (100 2Th.)	0.216 5	0.196 8	0.137 8	0.118 1
FWHM (101 2Th.)	0.472 3	0.393 6	0.159 7	0.157 4

Table 2 Selectivity of crystal growth directions for  $\text{Ni}(\text{OH})_2$  with different aging times

	Aging time / h	$D / \text{nm}$	$\Delta D / \Delta t / (\text{nm} \cdot \text{h}^{-1})$
(100)	3	0.660 2	0.220 0
	6	0.726 4	0.022 0
	9	1.037 0	0.103 5
	12	1.210 2	0.057 7
(101)	3	0.306 8	0.102 2
	6	0.368 1	0.020 4
	9	0.907 8	0.179 9
	12	0.920 6	0.004 2

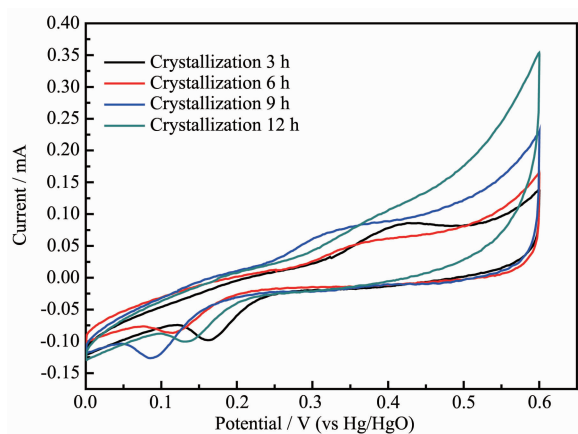


Fig.7 CV curves of the samples with different aging times

that with the increase of the aging time, the electrochemically active specific surface area also increases. When the aging time is 12 h, the electrochemically active specific surface area and peak current reach the maximum, which shows the best electrochemical activity. Therefore, it can be determined that the aging time is proportional to the electrochemical activity of  $\text{Ni}(\text{OH})_2$  crystal.

According to SEM analysis and CV analysis, the aging time has a influence on the morphology and electrochemical activity. Therefore, the relationship between the morphology and electrochemical activity can be determined: the higher sphericity leads to the better electrochemical activity, and the surface structure of striped micro-crystals has a better electrochemical activity than the surface structure of grainy micro-crystals.

Bulk density is one of the most important electrochemical indices of spherical  $\text{Ni}(\text{OH})_2$ . The bulk density of spherical  $\text{Ni}(\text{OH})_2$  determines the compactness of Ni electrode, and then affects the specific capacity. The international standard GB 1482-84 was applied in this experiment. And the bulk densities of the samples with different aging times are given in Table 3. It can be seen that the bulk density increases with the increase of the aging time, and it suggests that the aging time is proportional to the electrochemical activity of  $\text{Ni}(\text{OH})_2$  crystal, which is in agreement with CV analysis. Moreover, Fig.8 can lead to the mathematical relationship between the bulk

Table 3 Bulk densities of the samples with different aging times

Time / h	Bulk density / ( $\text{g} \cdot \text{mL}^{-1}$ )
3	0.49
6	0.92
9	1.44
12	1.75

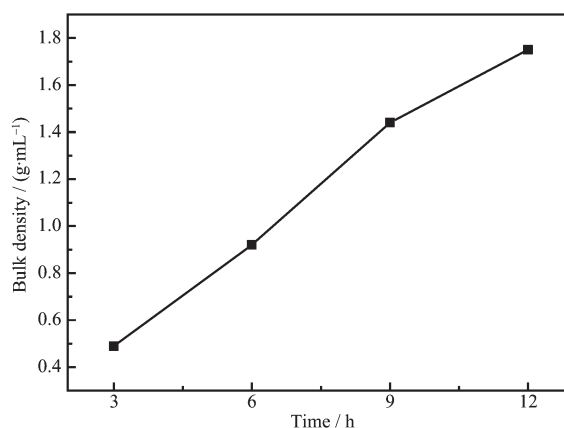


Fig.8 Aging time-conversion relation of bulk density

density and the aging time:  $d_s = 0.174T^{0.938}$ .

### 3 Conclusions

(1) Under the same physical and chemical conditions, the sphericity and the relative crystallinity of  $\text{Ni}(\text{OH})_2$  particles are proportional to the aging time. The mathematical relationship between aging time and amorphization is  $A = -0.0077T^2 + 0.0371T + 0.6532$ .

(2) Under the same physical and chemical conditions, the growth of (101) crystal plane has a greater influence on the sphericity of  $\text{Ni}(\text{OH})_2$  crystal than (100) crystal plane and contrary to the surface structure.

(3) Under the same physical and chemical conditions, the bulk densities increase with the increase of the aging time. The mathematical relationship between the bulk density and the aging time is  $d_s = 0.174T^{0.938}$ .

(4) The aging time is proportional to the electrochemical activity of spherical  $\text{Ni}(\text{OH})_2$ .

### References:

- [1] WANG Ji-Yang(王继洋). *Physics(物理)*, **2001**,6:332-339
- [2] FENG Shi-Hong(冯世宏), JIA Tai-Xuan(贾太轩), DU Hui-Ling(杜慧玲), et al. *Non-Ferrous Min. Metall.(有色矿冶)*, **2004**,20(5):48-50

- [3] Ma C Y, Liu J J, Wang X Z. *Particuology*, **2016**,**2**:1-18
- [4] Lee C H, Lee C H. *Korean J. Chem. Eng.*, **2005**,**22**:712-716
- [5] Huo Y, Liu T, Liu H, et al. *Chem. Eng. Sci.*, **2016**:126-139
- [6] Bagheri G H, Bonadonna C, Manzella I, et al. *Powder Technol.*, **2015**,**270**:141-153
- [7] Borchert C, Sundmacher K. *Chem. Eng. Technol.*, **2011**,**34**:545-556
- [8] Ramesh T N. *J. Phys. Chem. B*, **2009**,**113**:13014-13017
- [9] Deschamps J R. *Life Sci.*, **2010**,**86**:585-589
- [10] Deschamps J R, George C. *Trends Anal. Chem.*, **2003**,**22**:561-564
- [11] Cachau R E, Podjarny A D. *J. Mol. Recognit.*, **2005**,**18**:196-202
- [12] Wouters J, Ooms F. *Curr. Pharm. Des.*, **2001**,**7**:529-545
- [13] Blundell T L, Jhoti H, Abell C. *Nat. Rev. Drug Discovery*, **2002**,**1**:45-54
- [14] XU Gang(许岗), LI Ying-Jun(李英俊), GU Zhi(谷智), et al. *Chinese J. Inorg. Chem.*(无机化学学报), **2016**,**32**(7):1135-1140
- [15] Su Q F, Shi W M, Li D M, et al. *Nucl. Instrum. Methods Phys. Res. Sect. A*, **2011**,**659**:299-301
- [16] TANG Jun-Jie(唐俊杰), LIU Yan(刘燕), TIAN Lei(田磊), et al. *Chinese J. Inorg. Chem.*(无机化学学报), **2016**,**32**(7):1127-1134